Available online at www.sciencedirect.com
SCIENCE DIRECT®
PERGAMON
International Journal of Heat and Mass Transfer 46 (2003) 4335–4343
International Journal of HEAT and MASS TRANSFER
www.elsevier.com/locate/ijhmt

Axial solids mixing in a circulating fluidized bed

Yu.S. Teplitsky *, V.A. Borodulya, E.F. Nogotov

A.V. Luikov Heat and Mass Transfer Institute, Minsk, Belarus

Received 24 September 2002

Abstract

A phenomenological model of axial solids mixing in a circulating fluidized bed is formulated. The model allows for main specific features of the process: ascending motion of particles in the core zone and their descending motion in the annular zone (inner circulation of solids); substantial changes of particle concentration, sizes of core and annular zones over the bed height; net circulation of solids and the effect of the bottom bed on the process. The validity of initial postulates is confirmed by comparison of calculated and experimental curves of mixing.

1. Introduction

At present the technology of a circulating fluidized bed (CFB) is widely used in industry and power engineering [1,2]. Due to comparatively small time of research, main regularities of heat and mass transfer in CFB have not been studied adequately which makes development and designing of new large-scale apparatuses with CFB difficult. This refers, to a full extent, to solids mixing the studies of which are of practical importance for processes where continuous treatment of particles (drying, firing, combustion, etc.) is implemented or these particles gradually change their characteristics and require replacement (catalyst poisoning). Moreover, the character of solids mixing due to their 1000-fold higher bulk heat capacity, as compared with gas, determines the mechanism of heat transfer and leveling of temperatures in the apparatus.

By virtue of known [1] special features of CFB and its inner hydrodynamics (substantial nonuniformity of particle concentration both over the riser height and in their horizontal cross-section, intense inner circulation of solids, etc.), the process of solids mixing in this system is rather complex for both experimental study and its mathematical modeling. Now, the literature contains only fragmentary data on the laws governing the process which is insufficient for quantitatively, and often qualitative, evaluation of the effect of different factors on the intensity of solids mixing. The main difficulty of investigations is in correct interpretation of the obtained experimental data which is directly connected with a rational choice of the physical model of the process.

The simplest one-zone model with the only parameter—axial solids dispersion coefficient—was used in [3] for analysis of experimental solids residence time distributions in CFB with a diameter 0.152 and 0.305 m. A two-parameter model, which involves the particle velocity and axial solids dispersion coefficient, was used in [4] for analysis of the experiments on mixing of particles in CFB with a diameter 0.14 m. The authors do not give recommendations for determination of particle velocity. In [5], a more complex two-parameter two-dimensional (along the coordinates r and x) model which allows for a real structure of particle flows in CFB (ascending motion in the core zone and descending motion near the riser walls) and radial solids dispersion. The model considered a partial case of constant concentration of particles over the riser height, which considerable limited the range of its use. In [6], a rather complex multiparameter circulation model of solids mixing is suggested; the model directly allows for the two-zone structure of CFB. A considerable drawback of the model is in incorrect writing of diffusion and exchange terms which do not disappear at large times when the process of mixing ends and $c_1 = c_2 = c_\infty$. It should be noted that this refers, to the same measure, to the above-mentioned models where the form of presentation of diffusion terms follows from the Fick law for systems

* Corresponding author.
E-mail address: dsl@hmti.ac.by (Yu.S. Teplitsky).

0017-9310/$ - see front matter © 2003 Elsevier Ltd. All rights reserved.
doi:10.1016/S0017-9310(03)00242-4

Nomenclature

A	part of the horizontal cross-section of the riser occupied by ascending particles (the core zone)
B	part of the horizontal cross-section of the riser occupied by descending particles (annular zone)
$c_1 = c_1^*/\rho_1$ and $c_2 = c_2^*/\rho_2$	dimensionless concentrations of marked particles in the core zone and the annular zone
c_1^*, c_2^*	concentrations of marked particles in the core zone and the annular zone
c_0	initial dimensionless concentration of marked particles in $x = H_0$
$c = Ac_1 + Bc_2$	mean dimensionless concentration of marked particles
c_∞	$\lim_{t\to\infty} c$
D	$(pl/\rho^2)(u_1u_2/\beta_*)$
D_∞	$\lim D(u_1 \to \infty, u_2 \to \infty, \beta_* \to \infty)$
D_1, D_2, E	axial solids despersion coefficients
$Fr_t = (u-u_t)^2/gH$	Froude number
g	free-fall acceleration
H	riser height
H_0	height of the bottom bed
H_0'	H_0/H
j_i	diffusion flow of marked particles
J_s	net solids flow
$\overline{J}_s = J_s/\rho_s(u-u_t)$	dimensionless net solids flow
l	$B\rho_2$
p	$A\rho_1$
$Pe_c = (u-u_t)/\beta_* H$	Peclet numbers
$Pe_d = (u-u_t)H/E$	
$\overline{Pe}_c = Pe_c/\left(1 + 0.82(u_1'u_2'/(u_1'+u_2'))Pe_c(1/x')\right)$	
r	radial coordinate
t	time
$t' = t(u-u_t)/H$	dimensionless time
Δt	recirculation time (time interval between escape of particles from the upper part of the riser to entry to its base)
$\Delta t'$	$\Delta t(u-u_t)/H$
t_d'	$t_d(u-u_t)/H$
Δt_r	time in which the particles in the core zone pass the part of the riser from $x = H_0$ to $x = H$
T	$\Delta t_r + \Delta t$ recirculation period
T'	$T(u-u_t)/H$
u	superficial gas velocity
u_t	single-particle terminal velocity
u_1, u_2	velocities or particles in the core zone and the annular zone
u_1'	$u_1/(u-u_t), u_2' = u_2/(u-u_t)$,
x	vertical coordinate
x'	x/H

Greek symbols

β_*	exchange coefficient
β_1	coefficient introduced in (11)
$\underline{\beta}$	$\beta_*\rho$
$\overline{\beta}$	$\beta + p\beta_1$
ε	porosity
ρ_1, ρ_2	densities of the bed in the core and annular zones
ρ	$A\rho_1 + B\rho_2$ mean (over the horizontal cross-section of the bed) density of the bed
ρ_s	density of particles

Subscripts

1	core zone
2	annular zone
c	circulation model (35)–(37)
d	diffusion in Eqs. (44), (45), delay
fb	fluidized bed near the gas distributor (bottom bed)
r	radial
s	solids
t	conditions of floating of an single particle.

with constant density. Since, as is known, CFB is a system where density changes substantially in both horizontal ad vertical directions, the fact mentioned greatly restricts the applicability range of these models.

2. Phenomenological solids mixing model

The main assumptions which form the basis of the model are the following:

1. Ascending particle motion with velocity u_1 in the central part of the bed (core zone) and descending motion with velocity u_2 in the annular zone form inner circulation of the solid phase (Fig. 1). The following formulas are used for calculation of these velocities [7,8]

$$u_1 = u - u_t \quad [7], \tag{1}$$

$$u_2 = 0.1(u-u_t)Fr_t^{-0.7} \quad [8]. \tag{2}$$

As is seen, velocities u_1 and u_2 are constant over the bed height.

2. The existence of outer (net) circulation of solids, which is produced by solids flow J_s escaping from the upper part of the riser and then coming back to the bed base, is taken into account (Fig. 1).

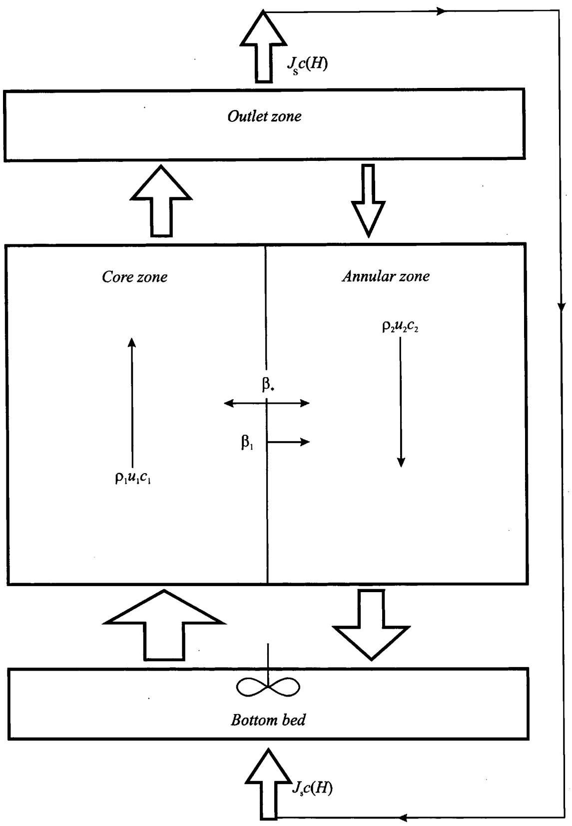

Fig. 1. Model of axial solids mixing in CFB.

3. In each horizontal cross-section of the riser there holds the equality

$$J_s = A\rho_1 u_1 - B\rho_2 u_2, \tag{3}$$

which determines a value of the specific circulating particle flow J_s (constant over the bed height and determining the intensity of net circulation of solids).
4. Local concentrations of particles in core zone (ρ_1) and annular zone (ρ_2) are linked by the correlation

$$\rho_2 = n\rho_1, \tag{4}$$

where n is the constant coefficient. By the data of [9], $n \simeq 2$–3.
5. A mean (over the horizontal cross-section of the riser) density of the bed $\rho = A\rho_1 + B\rho_2$ is variable over the height and is described by an empirical formula [10]:

$$\frac{\rho}{\rho_s} = \overline{J}_s (x')^{-0.82}, \quad H_0' \leqslant x' \leqslant 1. \tag{5}$$

6. Relative parts of the core zone (A) and the annular zone (B) change with the height, here in any horizontal cross-section of the bed

$$A + B = 1 \tag{6}$$

Formulas for calculation of A and B can be easily obtained from (3)–(6):

$$A = n\frac{u_2' + (x')^{0.82}}{u_1' + nu_2' - (x')^{0.82}(1-n)}, \tag{7}$$

$$B = \frac{u_1' - (x')^{0.82}}{u_1' + nu_2' - (x')^{0.82}(1-n)}, \tag{8}$$

for $H' \leqslant x' \leqslant 1$.
7. In the lower part of the bed there exists a zone with constant density and ideal mixing of particles—bottom bed (Fig. 1). Its height is calculated by [11]

$$H_0' = 1.25 Fr_t^{-0.8} \overline{J}_s^{1.1}. \tag{9}$$

By the data of [12], bottom bed porosity weakly depends on the velocity of gas and is a rather stable quantity.
In [11], it is suggested to determine it by the formula

$$\varepsilon_{fb} = 1 - 0.33 Fr_t^{-0.045}, \tag{10}$$

8. Particle exchange occurs between the core and annular zones. The exchange coefficient β_* is taken to be independent of the vertical coordinate x.
9. Dispersion transfer of marked particles with the coefficients D_1 and D_2 takes place in the core and annular zones, respectively, in addition to convective transfer.
10. Changes of the characteristics of CFB in horizontal direction are neglected.

We first write the continuity equations for solids in the core zone and annular zones

$$\frac{\partial A\rho_1}{\partial t} + u_1 \frac{\partial A\rho_1}{\partial x} = -A\beta_1\rho_1, \tag{11}$$

$$\frac{\partial B\rho_2}{\partial t} - u_2 \frac{\partial B\rho_2}{\partial x} = A\beta_1\rho_1. \tag{12}$$

The quantity $A\beta_1\rho_1$ [1] allows for (within the framework of the one-dimensional model) the existence of a radial particle flow J_r from the core zone to the annular zone (Fig. 2), which provides the experimentally observed decrease of densities ρ_1 and ρ_2 with a height at practically constant velocities u_1 and u_2.

Having summed (11) and (12), with account for (3) we obtain the continuity equation for the flow of outer circulation of solids

[1] In this case, a specific form of this quantity is not of principal value, since in what follows we use only the equality $A\beta_1\rho_1 = -u_1(\partial A\rho_1/\partial x)$ which follows from (11) under stationary conditions.

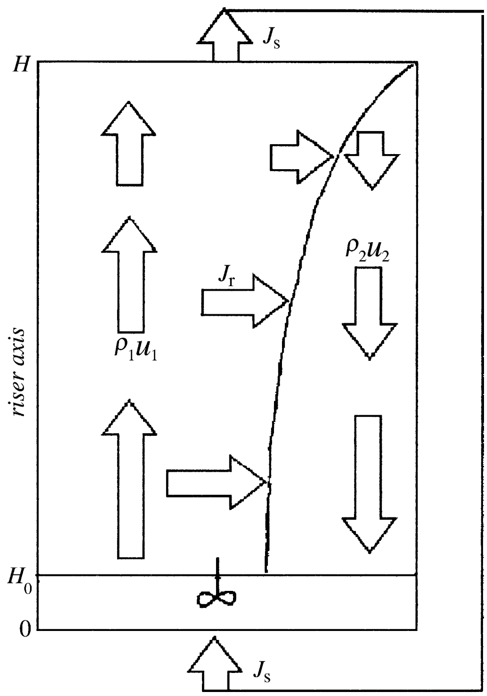

Fig. 2. Schematic of particle flows in CFB.

$$\frac{\partial \rho}{\partial t} + \frac{\partial J_s}{\partial x} = 0, \tag{13}$$

which leads to constancy of J_s under stationary conditions.

Taking the above assumptions into account, we formulate the system of equations which describe axial solids mixing in the CFB riser:

the core zone

$$\frac{\partial A\rho_1 c_1}{\partial t} + u_1 \frac{\partial A\rho_1 c_1}{\partial x} = \frac{\partial}{\partial x}\left(A\rho_1 D_1 \frac{\partial c_1}{\partial x}\right) + \beta_* \rho (c_2 - c_1) - A\rho_1 \beta_1 c_1, \tag{14}$$

the annular zone

$$\frac{\partial B\rho_2 c_2}{\partial t} - u_2 \frac{\partial B\rho_2 c_2}{\partial x} = \frac{\partial}{\partial x}\left(B\rho_2 D_2 \frac{\partial c_2}{\partial x}\right) + \beta_* \rho (c_1 - c_2) + A\rho_1 \beta_1 c_1. \tag{15}$$

The form of the diffusion terms in (14) and (15) corresponds to the Fick law in medium with a variable density [13]

$$j_i = -\rho_i D_i \frac{\partial c_i}{\partial x}, \quad i = 1, 2. \tag{16}$$

The contribution of these terms is likely to be estimated by the quantity $1/\widetilde{Pe} = \widetilde{D}/(u - u_t)H$, where $\widetilde{D}$ is the coefficient of the order of D_1 and D_2. With account for the fact that $\widetilde{D} \cong 10^{-3}$ m^2/s [1, p. 345], we have the estimate for $1/\widetilde{Pe}$: $1/\widetilde{Pe} \simeq 0.2 \times 10^{-4}$ at $H = 10$ m and $u - u_t = 5$ m/s which indicates that the share of diffusion terms in (14) and (15) is negligibly small. Taking this fact and the continuity equations (11) and (12) into account, we can represent the system of equations (14) and (15) as

$$A\rho_1 \frac{\partial c_1}{\partial t} + A\rho_1 u_1 \frac{\partial c_1}{\partial x} = \beta_* \rho (c_2 - c_1), \tag{17}$$

$$B\rho_2 \frac{\partial c_2}{\partial t} - B\rho_2 u_2 \frac{\partial c_2}{\partial x} = (\beta_* \rho + A\rho_1 \beta_1)(c_1 - c_2). \tag{18}$$

Despite the seeming simplicity, the system of equations (17), (18) has a rich essence and reflects virtually all important aspects of axial solids mixing in CFB.

For further analysis we introduce the notation: $p = A\rho_1$; $l = B\rho_2$; $\beta = \beta_* \rho$; $\overline{\beta} = \beta + A\rho_1 \beta_1$. Eliminating in turn c_1 and c_2 from (17) and (18), we reduce these equations to the form

$$\left(1 + \frac{p}{l}\frac{\overline{\beta}}{\beta} - u_2 \frac{\partial}{\partial x}\left(\frac{p}{\beta}\right)\right)\frac{\partial c_1}{\partial t} + \left(\frac{p}{l}\frac{\overline{\beta}}{\beta}u_1 - u_2 - u_1 u_2 \frac{\partial}{\partial x}\left(\frac{p}{\beta}\right)\right)\frac{\partial c_1}{\partial x} + \frac{p}{\beta}\frac{\partial^2 c_1}{\partial t^2} + \frac{p}{\beta}(u_1 - u_2)\frac{\partial^2 c_1}{\partial t\,\partial x} - \frac{p}{\beta}u_1 u_2 \frac{\partial^2 c_1}{\partial x^2} = 0, \tag{19}$$

$$\left(1 + \frac{l}{p}\frac{\beta}{\overline{\beta}} + u_1 \frac{\partial}{\partial x}\left(\frac{l}{\overline{\beta}}\right)\right)\frac{\partial c_2}{\partial t} + \left(-\frac{l}{p}\frac{\beta}{\overline{\beta}}u_2 + u_1 - u_1 u_2 \frac{\partial}{\partial x}\left(\frac{l}{\overline{\beta}}\right)\right)\frac{\partial c_2}{\partial x} + \frac{l}{\overline{\beta}}\frac{\partial^2 c_2}{\partial t^2} + \frac{l}{\overline{\beta}}(u_1 - u_2)\frac{\partial^2 c_2}{\partial t\,\partial x} - \frac{l}{\overline{\beta}}u_1 u_2 \frac{\partial^2 c_2}{\partial x^2} = 0. \tag{20}$$

Eqs. (19) and (20) are the second-order hyperbolic equations. We consider the important partial cases.

1. *Large times*. As is shown in [14], when $t \geqslant 10/\beta_*$, it is admissible to neglect the terms with $\partial^2/\partial t^2$ and $\partial^2/\partial t\,\partial x$ in the equations of type (19) and (20).
   With this in mind, we obtain

$$\left(\rho - \frac{1}{u_1}\frac{\partial}{\partial x}(\rho D)\right)\frac{\partial c_1}{\partial t} + \left(J_s - \frac{\partial}{\partial x}(\rho D)\right)\frac{\partial c_1}{\partial x} = \rho D \frac{\partial^2 c_1}{\partial x^2}, \tag{21}$$

$$\left(\rho + \frac{1}{u_2}\frac{\partial}{\partial x}\left(\frac{\beta}{\overline{\beta}}\rho D\right)\right)\frac{\partial c_2}{\partial t} + \left(J_s - \frac{\partial}{\partial x}\left(\frac{\beta}{\overline{\beta}}\rho D\right)\right)\frac{\partial c_2}{\partial x} = \frac{\beta}{\overline{\beta}}\rho D \frac{\partial^2 c_2}{\partial x^2}, \tag{22}$$

where $D = (pl/\rho^2)(u_1 u_2/\beta_*)$. This coefficient can be treated as the coefficient of axial "Taylor" diffusion which exists in the systems with a nonuniform field of axial velocities and exchange of substance in a radial direction [15]. Eqs. (21) and (22) are the parabolic equations of nonstationary convective diffusion with variable coefficients of dispersion D and $(\beta/\overline{\beta})D$ in the core and the annular zones, respectively.

2. *Stationary conditions of mixing*. These conditions are realized, as is known, at constant supply and removal of marked particles. The case is described by the following equations:

$$\left(J_s - \frac{\partial}{\partial x}(\rho D)\right)\frac{\partial c_1}{\partial x} = \rho D\frac{\partial^2 c_1}{\partial x^2}, \tag{23}$$

$$\left(J_s - \frac{\partial}{\partial x}\left(\frac{\beta}{\overline{\beta}}\rho D\right)\right)\frac{\partial c_2}{\partial x} = \frac{\beta}{\overline{\beta}}\rho D\frac{\partial^2 c_2}{\partial x^2}. \tag{24}$$

3. *An infinitely large coefficient of exchange* β_*, at which any difference between the phases disappears. Here two cases are possible:
(a) $u_1, u_2 \to \infty$, then $\lim_{\beta_*\to\infty} plu_1u_2/\rho^2\beta_* = D_\infty < \infty$. The system of equations (19), (20) is reduced to the only equation

$$\rho\frac{\partial c}{\partial t} + \left(J_s - \frac{\partial}{\partial x}(\rho D_\infty)\right)\frac{\partial c}{\partial x} = \rho D_\infty\frac{\partial^2 c}{\partial x^2}, \tag{25}$$

which is the equation of convective diffusion with a variable coefficient of dispersion D_∞ in the medium with variable density ρ.
(b) $u_1, u_2 < \infty$, then $D_\infty = 0$ and it follows from (25)

$$\rho\frac{\partial c}{\partial t} + J_s\frac{\partial c}{\partial x} = 0. \tag{26}$$

Eq. (26) describes convective transfer of marked particles at a velocity J_s/ρ.

4. *The absence of exchange between the phases* ($\beta_* = 0$). In this case, the phases are as in "quasi-isolated" and only one-sided transfer of marked particles from the core zone to the annular zone by the flow J_r occurs (Fig. 2). The initial system (17) and (18) takes the form

$$\frac{\partial c_1}{\partial t} + u_1\frac{\partial c_1}{\partial x} = 0, \tag{27}$$

$$\frac{\partial c_2}{\partial t} - u_2\frac{\partial c_2}{\partial x} = \frac{p}{l}\beta_1(c_1 - c_2). \tag{28}$$

Eqs. (27) and (28) describe convective transfer of marked particles upward with a velocity u_1 (the core zone) and downward with a velocity u_2 (the annular zone).

3. Numerical modeling of axial solids mixing in CFB

The system of equations (17) and (18) was used for numerical modeling of mixing of marked particles introduced at the initial instant of time to the bottom bed (Fig. 1). Such introduction of marked particles is most often used in experiments. The corresponding boundary-value problem has the form

$$\frac{\partial c_1}{\partial t} + u_1\frac{\partial c_1}{\partial x} = \frac{\beta}{p}(c_2 - c_1), \tag{29}$$

$$\frac{\partial c_2}{\partial t} - u_2\frac{\partial c_2}{\partial x} = \frac{\overline{\beta}}{l}(c_1 - c_2). \tag{30}$$

The initial and boundary conditions are:

$$\begin{aligned} &c_1(0,x) = c_2(0,x) = 0, \quad c_1(0,H_0) = c_0,\\ &x = H : c_1 = c_2 = c \quad x = H_0: \end{aligned} \tag{31}$$

(a) $t \leqslant T : \rho_{fb}H_0(\partial c_1/\partial t) + pu_1c_1 - lu_2c_2 = 0;$
(b) $t > T : \rho_{fb}H_0(\partial c_1/\partial t) + pu_1c_1 - lu_2c_2 = J_sc(t - \Delta t, H).$ [2]

We note that the boundary condition at $x = H$ is the consequence of the equation

$$pu_1c_1 - lu_2c_2 = J_sc, \tag{32}$$

which is the balance of marked particle flows at the riser outlet provided that mixing of particles in the outlet zone is good (Fig. 1). The quantities p and l which enter into (29)–(31) are related to a mean density of the bed $\rho = p + l$. Allowing for this fact, we can easily obtain from (4), (7) and (8) the formulas for calculation of p and l

$$p = \rho\frac{A}{A + Bn} = \rho\frac{u_2' + (x')^{0.82}}{u_1' + u_2'}, \tag{33}$$

$$l = \rho\frac{Bn}{A + Bn} = \rho\frac{u_1' - (x')^{0.82}}{u_1' + u_2'}. \tag{34}$$

Using (33) and (34) we write the system of equations (29)–(31) in a dimensionless form

$$\frac{\partial c_1}{\partial t'} + u_1'\frac{\partial c_1}{\partial x'} = \frac{1}{Pe_c}\frac{u_1' + u_2'}{u_2' + (x')^{0.82}}(c_2 - c_1), \tag{35}$$

$$\frac{\partial c_2}{\partial t'} - u_2'\frac{\partial c_2}{\partial x'} = \frac{1}{\overline{Pe}_c}\frac{u_1' + u_2'}{u_1' - (x')^{0.82}}(c_1 - c_2). \tag{36}$$

The initial and boundary conditions

$$\begin{aligned} &c_1(0,x') = c_2(0,x') = 0,\\ &c_1(0,H_0') = c_0,\\ &c_1 = c_2 = c, \quad x' = 1,\\ &x' = H_0': \end{aligned} \tag{37}$$

[2] It is assumed that all particles escaping from the riser again reach CFB in time Δt. The absence of recirculation is likely to correspond the condition $\Delta t = \infty$ ($T = \infty$).

(a) $t' \leqslant T'$: $mH_0' \frac{\partial c_1}{\partial t'} + \frac{u_2' + (H_0')^{0.82}}{u_1' + u_2'} u_1' c_1 - \frac{u_1' - (H_0')^{0.82}}{u_1' + u_2'} u_2' c_2 = 0;$

(b) $t' > T'$: $mH_0' \frac{\partial c_1}{\partial t'} + \frac{u_2' + (H_0')^{0.82}}{u_1' + u_2'} u_1' c_1 - \frac{u_1' - (H_0')^{0.82}}{u_1' + u_2'} u_2' c_2 = (H_0')^{0.82} c(t' - \Delta t', 1).$

The quantity $m = \rho_{\text{fb}}/\rho(H_0)$ is calculated by the formula $m = 0.4 Fr_t^{-0.7}$ which follows from (5), (9), and (10). As is seen, the system of equations (35)–(37) involves only one unknown parameter—the exchange coefficient β_* which enters into the numbers Pe_c and $\overline{Pe}_c$.

The boundary-value problem (35)–(37) was solved numerically by the finite-difference method. An implicit scheme of first order of accuracy was used. The computational region $H_0' \leqslant x' \leqslant 1$ was divided to 1000 intervals. Fig. 3 presents calculation of the concentration of marked particles at the riser outlet ($c_1 = c_2 = c$) at different values of Pe_c. For simplicity, calculations are made for the case $\Delta t = 0$ (marked particles is instantly carried from the outlet point of the riser to the point of re-entry). The calculation for the case $Pe_c = 0$ is given in Appendix A. A stationary value of concentration c_∞ can be easily calculated by the formula

$$c_\infty = \frac{c_0}{1 + \frac{5.5}{m}((H_0')^{-0.18} - 1)}, \tag{38}$$

which follows from the equation of material balance of marked particles. Fig. 4 gives the comparison of the data calculated at $\Delta t = \infty$ and experimental data of [16] where the quantities c_1 and c_2 were measured at different points of the riser with a diameter 0.305 m. A value of β_* obtained by the least-squares method is equal to 0.07 s^{-1}. We note that the given mixing curves which correspond to $Pe_c = 0$ are calculated by the formula

$$c = c_0 \exp\left(-\frac{(H_0')^{-0.18}}{m}(t' - t_d') \right), \tag{39}$$

which is the solution of equation

$$\rho_{\text{fb}} H_0 \frac{dc}{dt} + J_s c = 0, \tag{40}$$

proceeding from the boundary condition (a) in (31) at $c_1 = c_2 = c$. According to Eq. (26) the time of particle arrival at the given point of the riser is here determined as

$$t_d = \frac{1}{J_s} \int_{H_0}^{x} \rho \, dx = \frac{5.5H}{u - u_t}((x')^{0.18} - (H_0')^{0.18}). \tag{41}$$

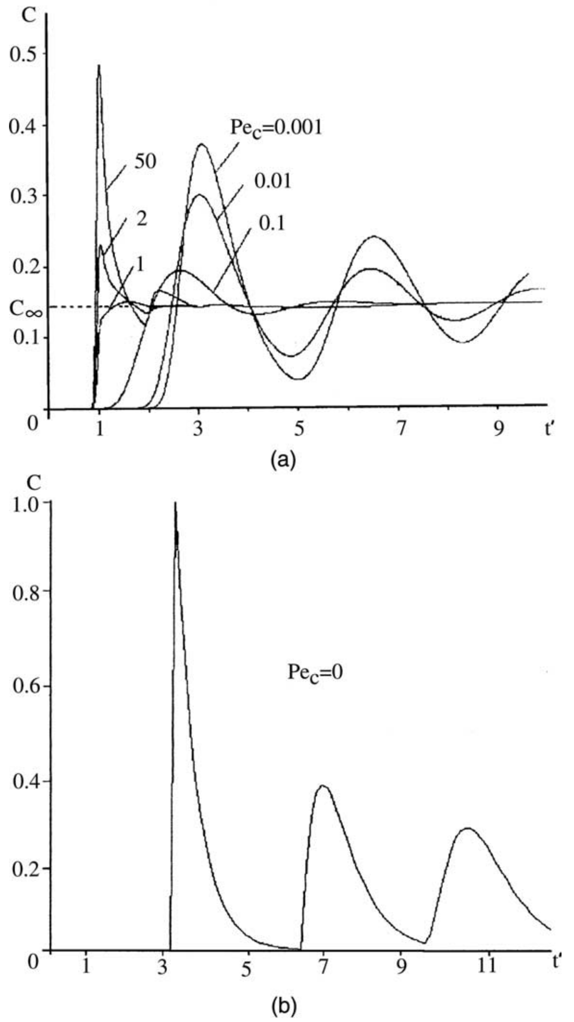

Fig. 3. Outlet curves of mixing for different values of Pe_c ($m = 1.208$, $H_0' = 0.01$, $c_\infty = 0.144$, $c_0 = 1$, $J_s = 50$ kg/m^2 s, $u = 6$ m/s, $H = 12$ m).

As is seen from Fig. 4, the calculated mixing curves are in good agreement with experimentally obtained values of concentrations c_1 and c_2 [16] and allow correct description of qualitative differences of the functions $c_1(t)$ and $c_2(t)$ which are observed in the experiment.

For comparison we considered a one-zone diffusion model with a constant axial solids dispersion coefficient E. The form of the equation is similar to (25):

$$\rho \frac{\partial c}{\partial t} + \left(J_s - \frac{\partial}{\partial x}(\rho E) \right) \frac{\partial c}{\partial x} = \rho E \frac{\partial^2 c}{\partial x^2}. \tag{42}$$

The initial and boundary conditions correspond to (31):

$$c(0, x) = 0; \quad c(0, H_0) = c_0; \qquad x = H, \quad \frac{\partial c}{\partial x} = 0, \quad x = H_0, \tag{43}$$

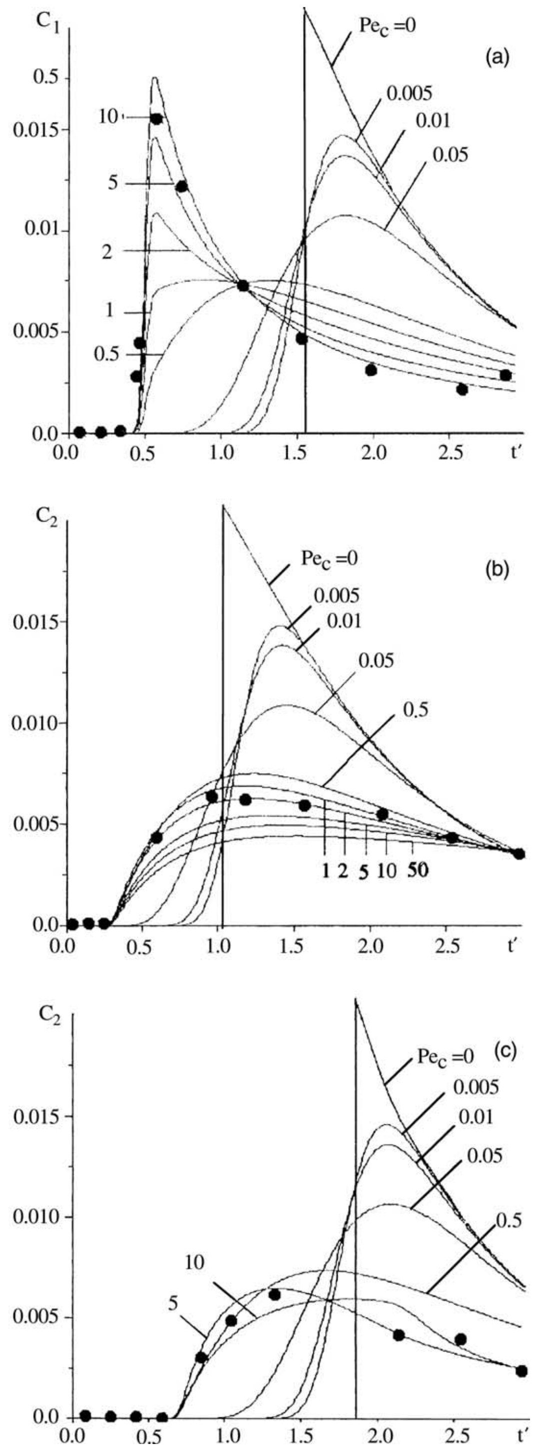

Fig. 4. Comparison of calculated mixing curves with experimental data [16]. (a) $x' = 0.55$, (b) $x' = 0.32$, (c) $x' = 0.75$. (●) Experimental points [16] ($m = 1.6$, $H_0' = 0.074$, $c_0 = 0.021$, $J_s = 147$ kg/m^2 s, $u = 4.57$ m/s, $H = 12.2$ m).

$$\text{(a)}\quad t \leqslant T: \quad \rho_{\text{fb}} H_0 \frac{\partial c}{\partial t} + J_s c - \rho E \frac{\partial c}{\partial x} = 0;$$

$$\text{(b)}\quad t > T: \quad \rho_{\text{fb}} H_0 \frac{\partial c}{\partial t} + J_s c - \rho E \frac{\partial c}{\partial x} = J_s c(t - \Delta t, H).$$

Using the expression for ρ from (5), we write the system of equations (42) and (43) in a dimensionless form

$$\frac{\partial c}{\partial t'} + \left((x')^{0.82} + \frac{0.82}{Pe_{\text{d}} x'} \right) \frac{\partial c}{\partial x'} = \frac{1}{Pe_{\text{d}}} \frac{\partial^2 c}{\partial (x')^2}. \tag{44}$$

The initial and boundary conditions are

$$c(0, x') = 0; \quad c(0, H_0') = c_0,$$
$$x' = 1; \quad \frac{\partial c}{\partial x'} = 0, \quad x' = H_0': \tag{45}$$

$$\text{(a)}\quad t' \leqslant T': \quad m H_0' \frac{\partial c}{\partial t'} + (H_0')^{0.82} c - \frac{1}{Pe_{\text{d}}} \frac{\partial c}{\partial x'} = 0;$$

$$\text{(b)}\quad t' > T': \quad m H_0' \frac{\partial c}{\partial t'} + (H_0')^{0.82} c - \frac{1}{Pe_{\text{d}}} \frac{\partial c}{\partial x'} = (H_0')^{0.82} c(t' - \Delta t', 1).$$

Fig. 5 presents the numerically obtained solutions of (44) and (45) for different values of Pe_{d} at the point $x' = 0.55$. It follows from comparison of Figs. 4 and 5:

1. The diffusion model is capable of describing the experimental data only at sufficiently large times ($t' \geqslant 1$). At small times, the diffusion model, in contrast to circulation one, cannot even give qualitative agreement with experimental data and describe different forms of the mixing curves in the core and annular zones.

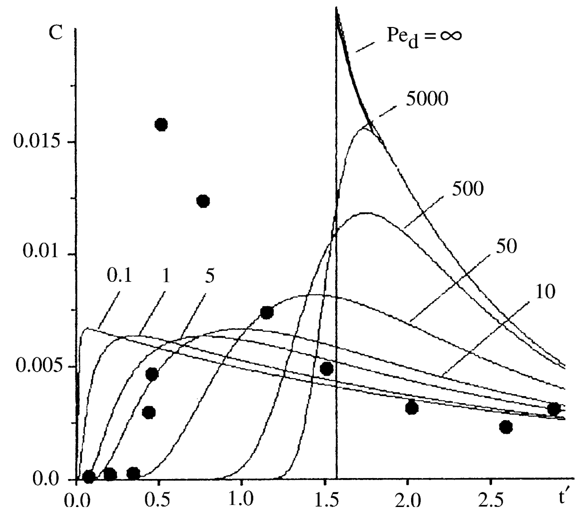

Fig. 5. Mixing curves calculated by the diffusion model at different values of the Pe_{d} number ($x' = 0.55$). (●) Experimental data [16] for concentration c_1.

2. The solutions of (44) and (45) at large Pe_d (small coefficients E) virtually coincide with the solutions of (35)–(37) at small Pe_c (large coefficients of exchange β_*). This corresponds to transition of Eq. (42) at small E to (26) and coincidence of the corresponding boundary conditions.

4. Conclusions

A two-zone model of axial solids mixing in CFB is formulated. The model allows for main special features of the process and, as is shown, is capable of satisfactory description the experimental mixing curves. The simplicity and comprehensive substation of Eqs. (17) and (18) make it possible to effectively use them for practical calculations.

Further investigations presuppose a detailed study of the dependence of the most important parameter of the model—the coefficient of exchange β_*—on the geometric (H, D) and hydrodynamic (J_s, u) characteristics of CFB.

Appendix A. The response function at the point $x' = 1$ at $Pe_c = 0$ (Fig. 3)

A dimensionless time of arrival of particles at the point $x' = 1$ (the delay time) t'_d is found from Eq. (41)

$$t'_d = 5.5\left(1 - (H'_0)^{0.18}\right) \cong 3.16. \quad \text{(A.1)}$$

Since the situation at the point $x' = 1$ exactly repeats the situation $x' = H'_0$ with delay $t'_d = \Delta t'_r$ (at $\Delta t' = 0$), the form of the response function at the CFB outlet can be easily obtained, with allowance for delay, from the solutions of the equations which describe two versions of the boundary condition at $x' = H'_0$ in (37). At $c_1 = c_2 = c$ and $\Delta t' = 0$ they have the form

$$\text{(a)} \quad t' \leqslant t'_d: \quad mH'_0 \frac{dc}{dt'} + c(H'_0)^{0.82} = 0, \quad \text{(A.2)}$$

$$\text{(b)} \quad t' > t'_d: \quad mH'_0 \frac{\partial c}{\partial t'} + c(H'_0)^{0.82} = (H'_0)^{0.82} c(t', 1). \quad \text{(A.3)}$$

The solution of Eq. (A.2) with the initial condition $c(t'_d) = c_0 = 1$ has the form

$$c(t') = \exp\left(-\frac{(H'_0)^{-0.18}}{m}(t' - t'_d)\right). \quad \text{(A.4)}$$

The function (A.4) describes the shape of the mixing curve at $x' = 1$ within the range of times $t'_d \leqslant t' \leqslant 2t'_d$ when the effect of solids recirculation does not begin to manifest itself. At larger times, one should use Eq. (A.3) which allows for recirculation of particles. Within the range of times $2t'_d \leqslant t' \leqslant 3'_d$ the form of the response function follows from the solution of Eq. (A.3), which, with account for (A.4) has the form

$$mH'_0 \frac{dc}{dt'} + c(H'_0)^{0.82} = (H'_0)^{0.82} \exp\left(-\frac{(H'_0)^{-0.18}}{m}(t' - 2t'_d)\right). \quad \text{(A.5)}$$

The role of the initial condition for (A.5) is played by the relation

$$c(2t'_d) = \exp\left(-\frac{(H'_0)^{-0.18}}{m} t'_d\right), \quad \text{(A.6)}$$

which follows from (A.4) at $t' = 2t'_d$. The solution of (A.5) and (A.6) has the form

$$c(t') = \frac{(H'_0)^{-0.18}}{m}(t' - 2t'_d) \exp\left(-\frac{(H'_0)^{-0.18}}{m}(t' - 2t'_d)\right) + \exp\left(-\frac{(H'_0)^{-0.18}}{m}(t' - t'_d)\right). \quad \text{(A.7)}$$

For the next period of time $3t'_d \leqslant t' \leqslant 4t'_d$ calculation of the response functions follows from the solution of equation

$$mH'_0 \frac{dc}{dt'} + c(H'_0)^{0.82} = (H'_0)^{0.82} \left(\frac{(H'_0)^{-0.18}}{m}(t' - 3t'_d) \times \exp\left(-\frac{(H'_0)^{-0.18}}{m}(t' - 3t'_d)\right) + \exp\left(-\frac{(H'_0)^{-0.18}}{m}(t' - 2t'_d)\right)\right), \quad \text{(A.8)}$$

with the initial condition following from (A.7) at $t' = 3t'_d$

$$c(3t'_d) = \frac{(H'_0)^{-0.18}}{m} t'_d \exp\left(-\frac{(H'_0)^{-0.18}}{m} t'_d\right) + \exp\left(-\frac{(H'_0)^{-0.18}}{m} 2t'_d\right) \quad \text{(A.9)}$$

The solution of (A.8) and (A.9) has the form

$$c(t') = \left(\left(\frac{(H'_0)^{-0.18}}{m}\right)^2 \frac{(t' - 3t'_d)^2}{2} + \frac{(H'_0)^{-0.18}}{m}(t' - 3t'_d) \times \exp\left(-\frac{(H'_0)^{-0.18}}{m} t'_d\right) + \frac{(H'_0)^{-0.18}}{m} t'_d \times \exp\left(-\frac{(H'_0)^{-0.18}}{m} t'_d\right) + \exp\left(-\frac{2(H'_0)^{-0.18}}{m} t'_d\right)\right) \times \exp\left(-\frac{(H'_0)^{-0.18}}{m}(t' - 3t'_d)\right) \quad \text{(A.10)}$$

Calculation of subsequent periods of time is similar. Fig. 3 shows the response function for $Pe_c = 0$ constructed by Eqs. (A.4), (A.7) and (A.10).

References

[1] A.P. Baskakov, Flow-through fluidized systems, in: V.G. Ainshtein, A.P. Baskakov (Eds.), Fluidization, Khimiya Press, Moscow, 1991, pp. 333–395.

[2] A.P. Baskakov, V.V. Matsnev, I.V. Raspopov, Boilers and Furnaces with Fluidized Bed, Energoatomizdat Press, Moscow, 1995.

[3] M. Rhodes, S. Zhou, T. Hirama, H. Cheng, Effects of operating conditions and scale on solids mixing in risers of circulating fluidized beds, in: O.E. Potter, D.J. Nicklin (Eds.), Proceedings of the 7th Engineering Foundation Conference on Fluidization, Bristane, Australia, 1992, pp. 249–256.

[4] D. Bai, J. Yi, Jin, Z. Ju, Residence time distributions of gas and solids in a circulating fluidized bed, in: O.E. Potter, D.J. Nicklin (Eds.), Proceedings of the 7th Engineering Foundation Conference on Fluidization, Bristane, Australia, 1992, pp. 195–202.

[5] G.S. Patience, J. Chaouki, Solids hydrodynamics in the fully developed region of CFB risers, in: Fluidization VIII Preprints, vol. 1, Tours, France, 1995, pp. 33–40.

[6] Q. Wang, J. Zhou, J. Tu, et al., Residence time in circulating fluidized bed, in: CFB-5 Preprints, Beijing, China, 1996, pp. DB 20 1–6.

[7] J. Werther, E.-U. Hartge, M. Kruse, Gas mixing and interphase mass transfer in the circulating fluidized bed, in: O.E. Potter, D.J. Nicklin (Eds.), Proceedings of the 7th Engineering Foundation Conference on Fluidization, Bristane, Australia, 1992, pp. 257–264.

[8] Yu.S. Teplitsky, Near-wall hydrodynamics of a circulating fluidized bed, Inzh.-Fiz. Zh. 74 (2001).

[9] W. Nowak, Comprehensive study of the circulating fluidized bed, Ass. Prof. Thesis, Czistochwa, 1989.

[10] V.A. Borodulya, Yu.S. Teplitsky, Scaling in a circulating bed, in: Proceedings of the 3rd Minsk International Forum, Minsk, Belarus, vol. 5, 1996, pp. 69–74.

[11] Yu.S. Teplitsky, V.I. Kovensky, Resistance of a circulation fluidized bed, Inzh.-Fiz. Zh. 74 (2001) 62–66.

[12] F. Johnsson, B. Leckner, Vertical distribution of solids in a CFB-furnace, in: Proceedings of the 13th International Confernec on Fluidized Bed Combustion, Orlando, Florida, 1995, pp. 1–9.

[13] B. Bird, W. Stewart, E. Lightfoot, Transport Phenomena, Moscow, 1974.

[14] Yu.S. Teplitsky, Hydrodynamics and heat transfer in free and retarded fluidized beds, Author's Abstract of Doctoral Thesis (in Engineering), Novosibirsk, 1990.

[15] G. Taylor, Dispersion of soluble matter in solvent flowing slowly through a tube, Proceedings of the Royal Society of London, Series A 219 (1953) 186–203.

[16] B. Bader, J. Findlay, T.M. Knowlton, Gas/solids flow patterns in a 30.5-cm-diameter circulating fluidized bed, in: P. Basu, J.F. Large (Eds.), Circulating Fluidized Bed Technology, Pergamon Press, Oxford, 1988, pp. 123–138.